Actinomycosis versus Tuberculosis in ancient Human Bone – a pilot study

Schamall D.[1,8], Haring E.[2], Nebot Valenzuela E.[3,4], Pietschmann P.[3], Tangl S.[5], Edelmayer M.[6], Dobsak T.[5], Krause J.[7], Spyrou M.[7], Teschler-Nicola M.[1,8]

[1] Department of Anthropology, University of Vienna, Vienna, Austria · [2] Central Research Laboratories, Natural History Museum Vienna, Vienna, Austria · [3] Department of Pathophysiology and Allergy Research, Centre for Pathophysiology, Infectiology and Immunology, Medical University of Vienna, Vienna, Austria · [4] Department of Physiology, School of Pharmacy, and Institute of Nutrition and Food Technology, University of Granada, Granada, Spain · [5] Karl Donath Laboratory, University Clinic of Dentistry Vienna, Vienna, Austria · [6] Department of Oral Surgery, University Clinic of Dentistry Vienna, Vienna, Austria · [7] Max Planck Institute for the Science of Human History, Jena, Germany · [8] Department of Anthropology, Natural History Museum Vienna, Vienna, Austria

Introduction

Actinomycosis is a rare chronic infectious disease hallmarked by extensive tissue destruction. It is caused by several known subspecies of Actinomycoses; these are anaerobic bacilli that regularly colonise the oropharyngeal cavity, bronchial system, and gastrointestinal tract. In few cases, especially in immunocompromised humans, the mucosal or epithelial barrier is breached and local abscesses infiltrate either the adjacent soft tissues or disseminate by vascular pathways.

An affection of bone tissue is very rare. In this pilot study one recent case with documented Actinomycosis is presented, and one historical case with assumed Actinomycosis is discussed.

Case presentations

A historically well documented case of Actinomycosis that concerns the vertebrae, sacrum, and pelvis of a 21-year-old female dated to the 19th century is examined (Figs. 1 and 2). This specimen was provided by the Pathological-anatomical Collection from the Natural History Museum Vienna. These remnants are compared with the controversially interpreted pathological alterations observed at the lumbar spine of a mature male skeleton recovered at the early Mediaeval Gars/Thunau site (Lower Austria) that hitherto is associated with a *M. tuberculosis* infection (Fig. 12).
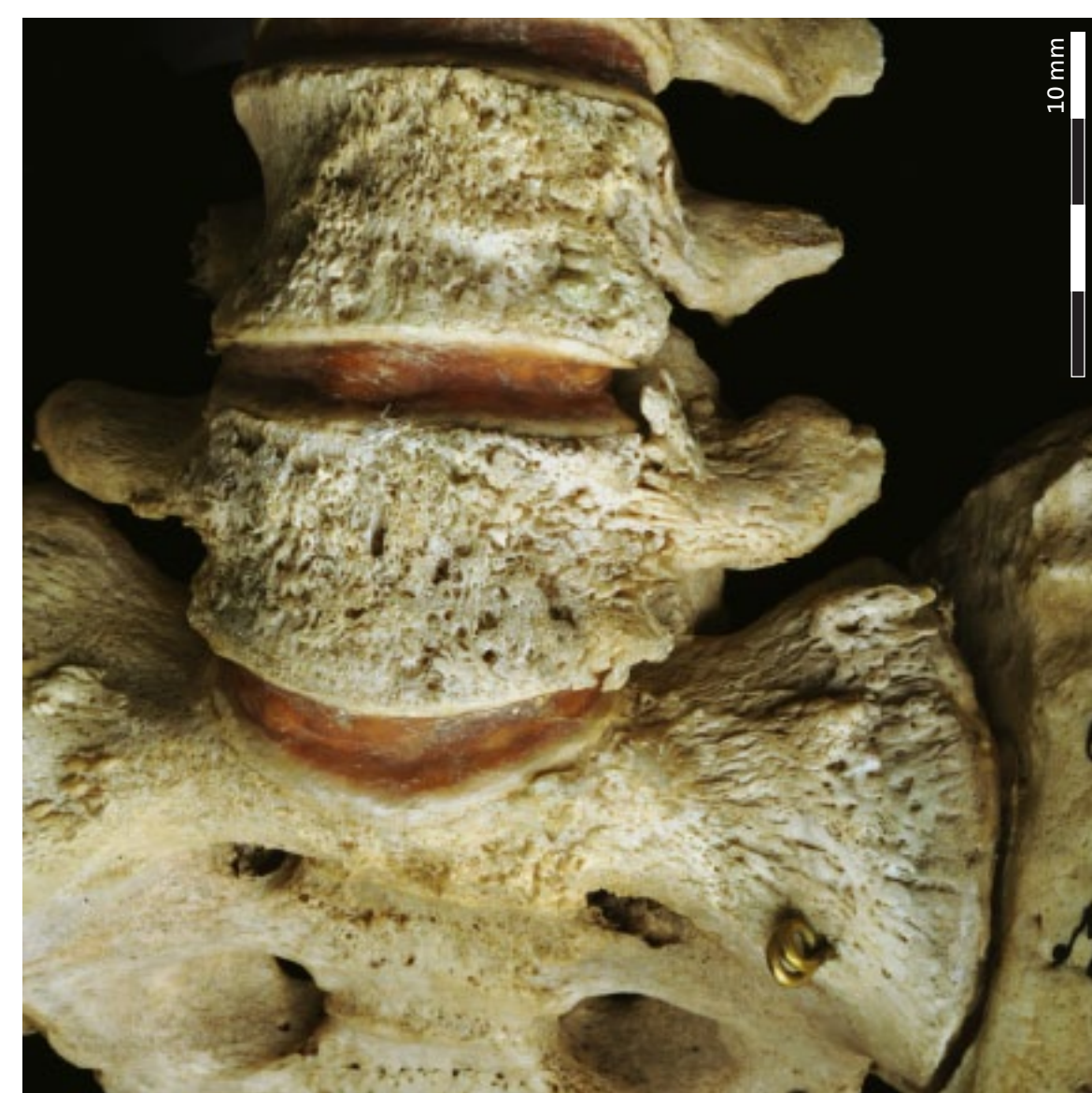
Methods

Following overall photographical and conventional radiological documentation, structural analyses and 3-D-reconstructions by an X-ray based μCT scanner (VISCOM X-8060-II) were performed on the spine and, additionally in the recent case, of the pelvis (transmission tube, digital detector, 110 kV, 380 μA, filter: 0.50 mm copper; spatial resolution: 40 μm; zoom factor: in a range between x3.0 to 3.3). The very badly preserved historical pelvis was not suitable for this examination. Subsequently, a cross section of the region around the *Spina iliaca anterior inferior* was sawed out from the recent pelvis and resin-embedded in Technovit. Then undecalcified thin-ground sections were prepared and stained by the method of Levai-Laczko. Finally, for aDNA analyses bone samples from areas presenting reactive bone formation were drilled out below the *Crista iliaca*, ventrally of the *Tuberositas iliaca*; these bone samples served as template for DNA extraction (Dabney et al. 2013). After extraction, each sample is turned into a DNA library (Meyer & Kircher 2010) and sequenced on a Next Generation Sequencing platform (work in progress). Post sequencing, the fast algorithm MALT (Herbig et al. 2016) will be used for assigning DNA reads to their respective source species (therefore identifying environmental bacteria associated with post-mortem colonisation, but most importantly endogenous microbiota as well as pathogenic bacteria that might be associated to the presented pathology).

Fig. 1: Macroscopical overview of the lower lumbar and upper sacral vertebrae (21-year-old female from the 19th century): note the reactive bone formation and numerous *Foramina* at the ventral side.

Fig. 2: Macroscopical overview of the left pelvis (21-year-old female): note the new periosteal bone deposition and also plenty of additional *Foramina* at the abdominal side.

Fig. 3: Radiograph of the lower lumbar vertebrae in lateral projection (21-year-old female): note the vascular channels at the anterior aspect of the vertebral bodies and the thinned cortical bone. However, the trabecular bone shows thickened and sclerotic elements, but there also are some bulked areas.
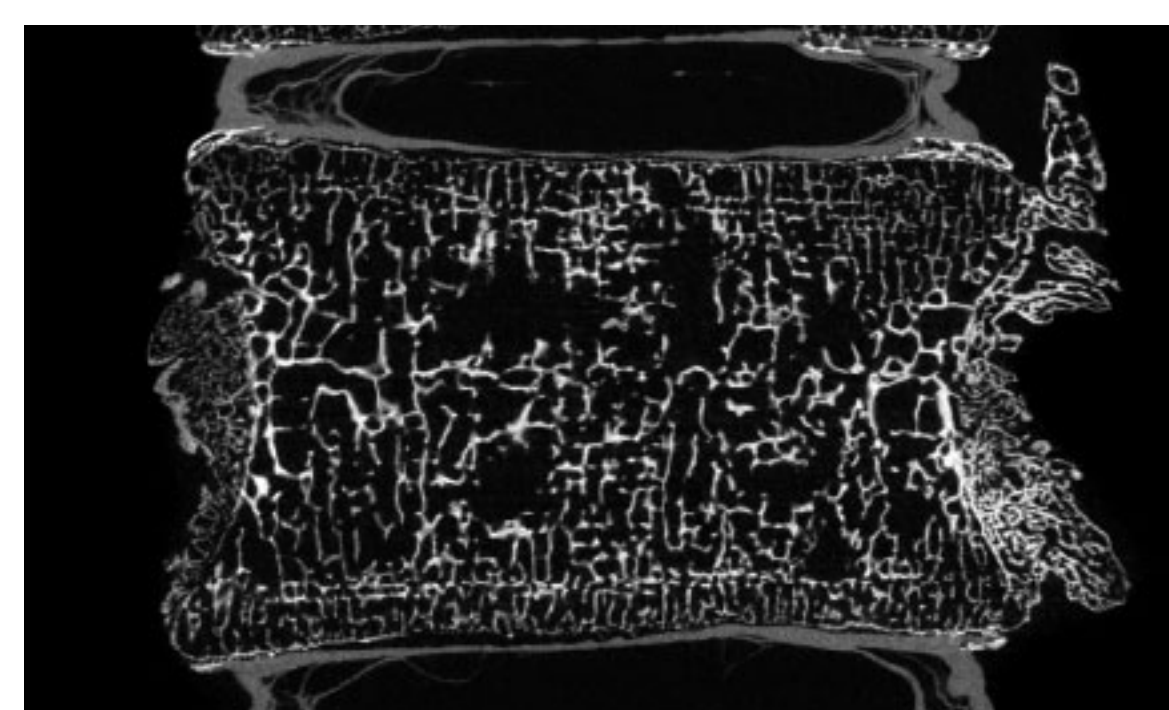

Fig. 4: Radiograph of the left pelvis in anteroposterior projection (21-year-old female): note the marked thickening of the *Iliac fossa* and the dense trabecular network within the reactive bone formation.

Fig. 5: μCT-image in frontal plane of the 5th lumbar vertebra: note the destructions within the vertebral body and the disaggregation of the cortical bone. However, the laterally new built bone shows lots of trabecular-like structures.

Fig. 10: Histological detail of the 5th vertebra: parallel fibered bone as part of the plexiform bone. Towards the periphery it is still actively growing as demonstrable by the presence of woven bone exclusively. Due to the lack of cement lines, there is no hint of remodelling in this area.
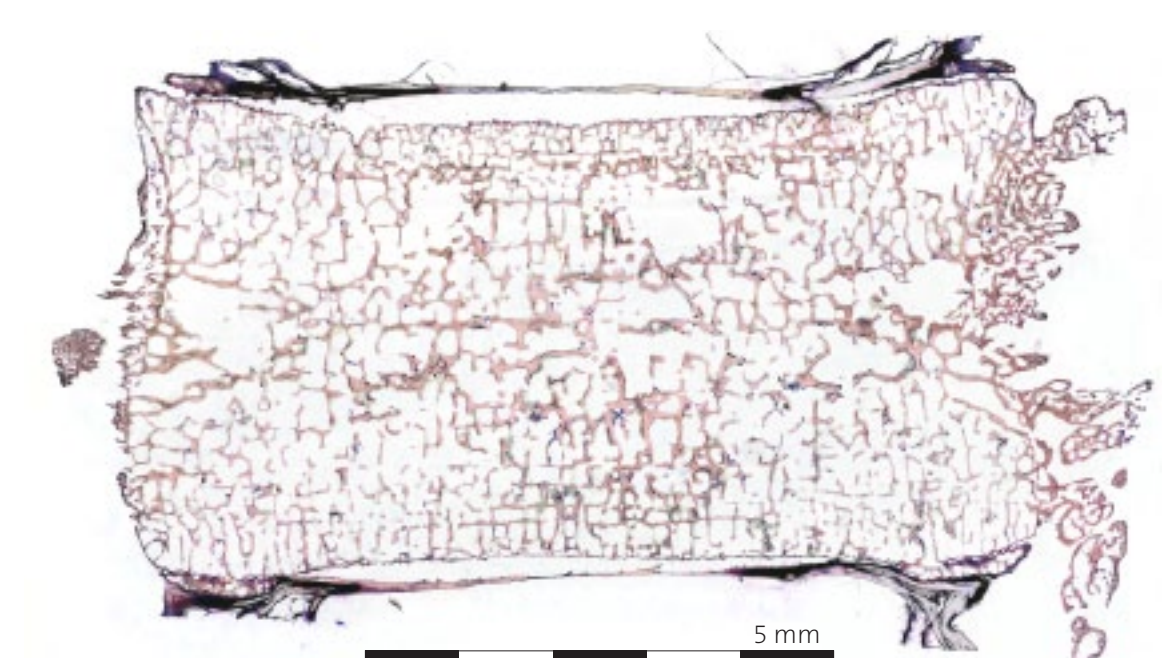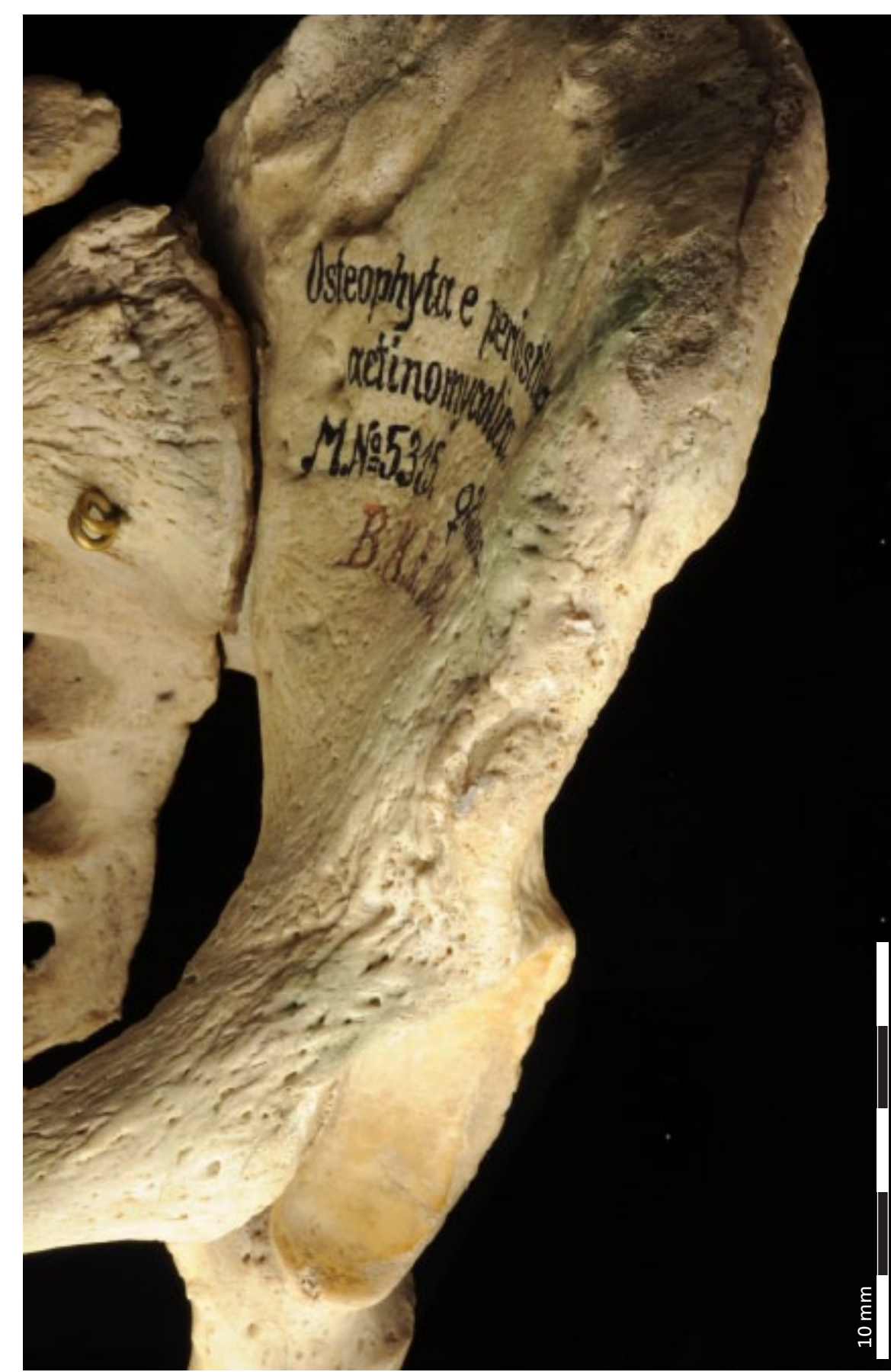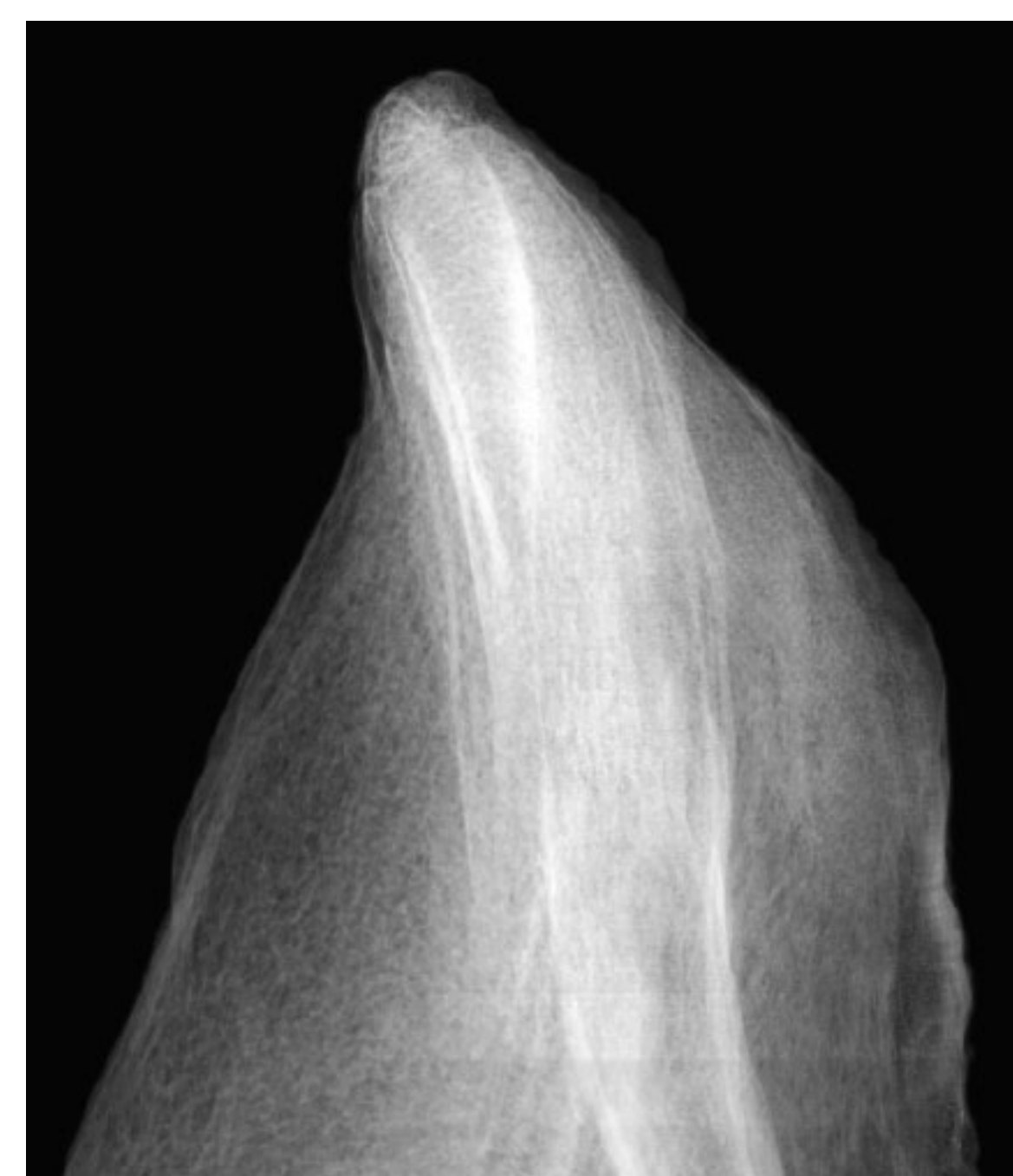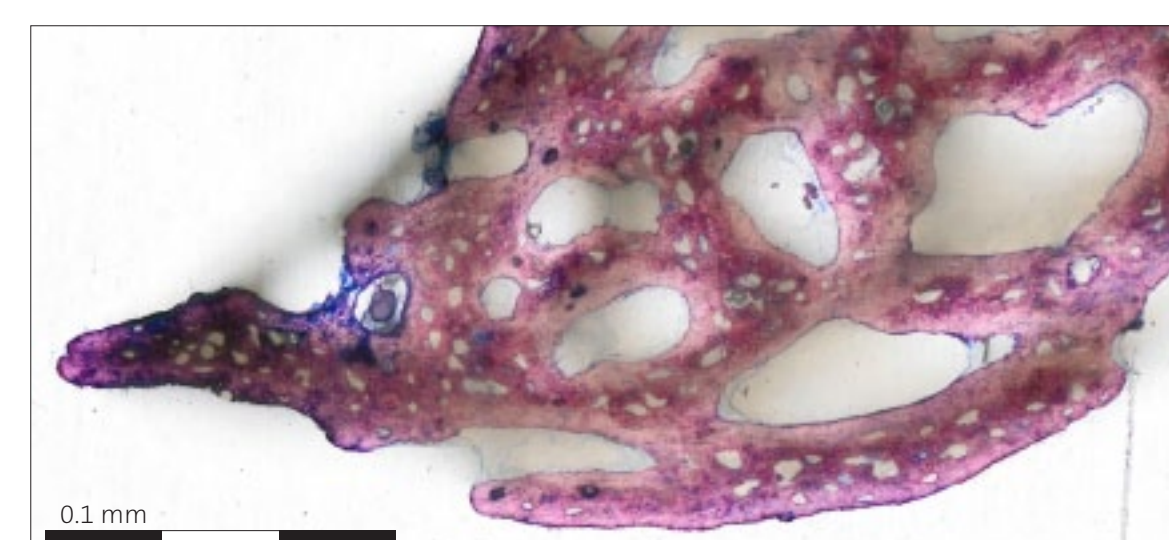

Fig. 9: Histological overview of the 5th vertebra in frontal plane: the new built structures are identified also to be plexiform bone, forming lateral extensions.

Fig. 6a: 3-D-reconstruction of μCT-images of the right pelvis: note the regular form and thickness. The black areas indicate the subsequent regions from the correspondent single μCT-planes (Figs. 6c, 6e, and 6g); the plotted red area represents the μCT-plane (Fig. 6i) that matches the histological thin-section (Fig. 7).

Fig. 6b: 3-D-reconstruction of μCT-images of the left pelvis: note the irregular form and pronounced thickening. The black areas indicate the subsequent regions from the correspondent single μCT-planes (Figs. 6d, 6f, and 6h); the plotted red area represents the μCT-plane (Fig. 6j) that matches the histological thin-section (Fig. 8).

Figs. 6c, 6e, and 6g: Single μCT planes in transversal orientation of the right pelvis: note the typical shape and structure of a flat bone.

Figs. 6d, 6f, and 6h: Single μCT planes in transversal orientation of the left pelvis: note the bulked and partly eroded cortical bone at both sides and the plexiform bone at the abdominal side.

Fig. 6i: Single μCT plane in transversal orientation of the right pelvis that matches the histological thin-section (Fig. 7): note the regular trabecular bone, whereas there are slight irregularities at the abdominal contour of the cortical bone.

Fig. 6j: Single μCT plane in transversal orientation of the left pelvis that matches the histological thin-section (Fig. 8): note the severe alterations at both cortices and the large amounts of plexiform bone at the abdominal side.

Fig. 7: Histological overview at the level of the anterior inferior iliac spine of the right pelvis shows predominantly regular lamellar bone except superficial erosion at the abdominal side of the cortical bone.

Fig. 8: Histological overview at the level of the anterior inferior iliac spine of the left pelvis reveals that the periosteal reactions consist of plexiform bone.

Results of the recent case

Macroscopically, the anterior surface of the lumbosacral spine and the left *Os ilium* are affected by extensive reactive bone formation at the periosteal side that is pierced by numerous *Foramina* (Figs. 1 and 2). Radiologically in lateral view, it can be proven that these *Foramina* lead to vascular channels. The vertebral cortical bone appears to be thinned, but intact. Within the vertebral body, especially in the 5th lumbar vertebra, the trabeculae exhibit signs of thickening and sclerotic alterations around some "holed" areas (Fig. 3). The left hip shows pronounced thickening at the abdominal side due to newly built bone, and a dense trabecular network within this bone formation that does not occur at the corresponding other side (Fig. 4). The 3-D-reconstruction of μCT-images in frontal plane of the 5th lumbar vertebra reveals gross excavations within an extended central third and even disaggregation of the cortical bone, whereas the laterally visible new built bone is very densely packed by trabecular-like structures (Fig. 5). The 3-D-reconstruction of μCT-images of the pelvis illustrates the regular configuration at the right side (Fig. 6a) and the strongly modified appearance at the left side (Fig. 6b). The μCTs in transversal plane of the pelvis show regular form and thickness at the right pelvis (Figs. 6c, 6e, and 6g), except slight irregularities at the cortex of the abdominal side at the level of the anterior inferior iliac spine (Fig. 6i), but the presence of definitely plexiform bone adjacent to the bulked and partly eroded cortex (Figs. 6d, 6f, 6h, and 6j). Histologically, the findings gained by μCT are confirmed and extended (Figs. 7, 8 and 9): All periosteal reactions are proved to be plexiform bone that already is remodelled close to the original bony contour, but towards the periphery is still actively growing (Fig. 10). Interestingly, there is also a superficial erosion of the cortical bone demonstrable at the macroscopically apparently not affected right side of the *Os ilium* (Fig. 7). Furthermore, some granulomatous structures are visible within the vertebra and the obviously affected left ilium that cannot be found on the right side (Figs. 11a and b). The molecular genetic analyses of aDNA are still not completed.

Discussion

Actinomycoses belong to the regular oral, pulmonary, and abdominal flora, but following any mucosal or epithelial damage, this barrier might be passed and a chronic purulent infection can develop that results in infiltrative inflammation (Ortner & Putschar 1981). Typically the bacterial pathogens concern the orocervicofacial (55 %), abdominopelvic (20 %), thoracic (15 %), and other (10 %) regions (Patil et al. 2014). Bone destructions result from a direct contact to the infected adjacent soft tissues and concern most often vertebrae, mandible and ribs, but also the pelvis. As the periosteal layer is involved, the symptoms include hypervascularisation, new bone formation, and destruction of cancellous bone mostly without sclerotic response (Ortner & Putschar 1981). Actinomycotic alterations in dry bone are rare and unspecific, thus, they can be misdiagnosed as malignancies (e.g., sarcomas), syphilitic (gummae), osteomyelitic (fistulae), and especially tuberculotic (abscess formation) lesions (Park et al. 2003, Patil et al. 2014).

Macroscopical as well as conventional radiological examination of the recent case show hypervascularisation and considerable new periosteal bone deposition in all skeletal elements, which is typical for Actinomycosis. Additionally, μCT-images reveal cortical impairment below the new bone formation without significant endosteal sclerotic response, also as described for this disease (e.g., Ortner & Putschar 1981). Moreover, 3-D-reconstructions and histological examinations prove the presence of plexiform bone, which is yet not reported to occur. This type of bone formation is known to be found in periods of rapid growth and is highly vascularised. The vascular channels are surrounded by woven bone that is first compacted by the apposition of parallel fibered bone and later gets substituted by lamellar bone. In the recent case, the outer subperiosteal areas still were actively growing and consist of woven bone only, whereas the inner segments were already partly remodelled and replaced by lamellar bone. Furthermore, remarkable granulomatous structures occurred within the medullary zones that differ from the regular medullary tissue. These might represent dehydrated bacterial remnants as they quite strongly resemble images from recent publications (Hansen et al. 2007) and are found in the vertebra and affected left pelvis, but not in the right one. To proof this assumption the aDNA analysis is currently carried out.

In contrast, the historic case is characterised by a wedge-shaped contour of the vertebrae (Fig. 13), a vast loss of trabecular bone, the absence of plexiform bone, and a huge extent of cavitary defects as well as fusion of the affected vertebrae (Fig. 12) suggest Tuberculosis rather than Actinomycosis. But because of the dense erosion of the cortical bone and reactive newly deposited bone on the vertebral endplates, that seems to be strongly vascularised (Fig. 14), any signs of sclerotic response with thickened trabeculae and the unchanged vertical general organisation of the trabeculae (Coquegniot et al 2015), as well as the lack of a secondary new bone layer covering the osteolytic lesions (Palfi et al. 2015), Actinomycosis cannot be excluded.
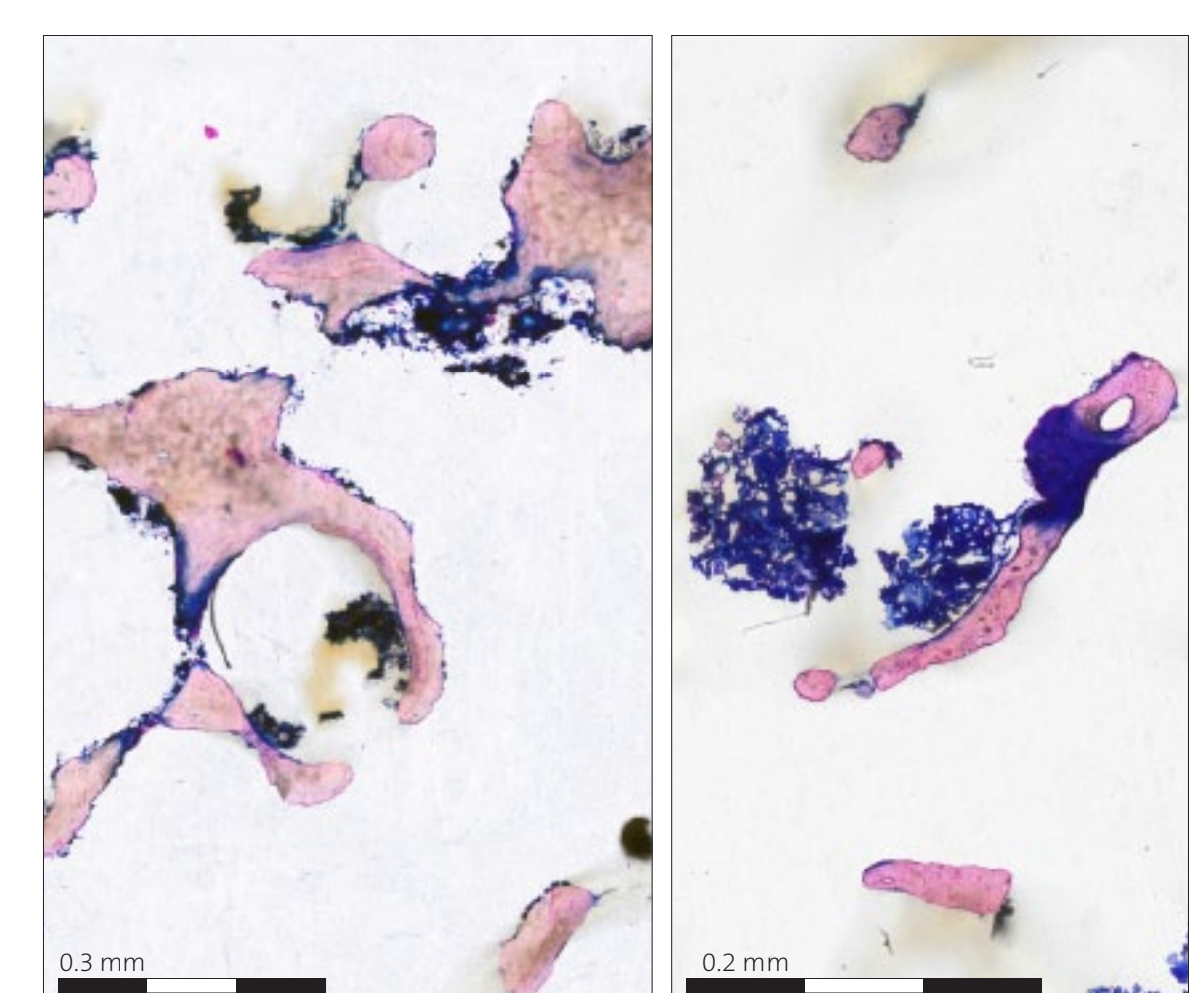
Fig. 11: Histological detail of the 5th vertebra (11a) and the left pelvis (11b): within the medullary zones granulomatous structures along the trabeculae occur that differ from the regular medullary tissue. Such structures cannot be found on the right pelvis.

Results of the mediaeval case

Macroscopically, huge cavitations on one hand, and extended new bone formations on the other hand – whose extensions even bridge to the upper vertebra – characterise the outer aspect of the strongly deformed vertebral bodies. Numerous *Foramina* perforate the newly built bone (Fig. 12). Radiologically in lateral view, cavitation even within the vertebral bodies are visible and a strongly coarsened trabecular pattern. Besides this, also hyperdense zones occur indicating some areas with sclerosis. The cortical bone is massively altered leading to a wedge-shaped form of the cone. The new bone formation on the outer anterior side is solid with only few hints of hypervascularity (Fig. 13). The μCT in frontal plane evinces the tremendous extent of trabecular rarefication whereas the "sclerotic" areas turn out to be of post mortal origin. The cortex becomes eroded and even split to several thin layers, but not as in plexiform bone. The new bone formation is very densely packed by irregularly arranged trabeculae (Fig. 14).

Literature

Coquegniot H., Dutailly B., Desbarats P., Boulestin B., Pap I., Szikossy I., Baker O., Montaudon M., Panuel M., Karlinger K., Kovacs B., Kristof L.A., Palfi G., Dutour O. (2015): Three-dimensional imaging of past skeletal TB: From lesion to process. Tuberculosis, 95: S73–S79.

Dabney J., Knapp M., Glocke I., Gansauge M.T., Weihmann A., Nickel B., Valdiosera C., Garcia N., Pääbo S., Arsuaga J.L., et al. (2013): Complete mitochondrial genome sequence of a Middle Pleistocene cave bear reconstructed from ultrashort DNA fragments. Proceedings of the National Academy of Sciences of the United States of America, 110: 15758–15763.

Hansen T., Kunkel M., Springer E., Walter C., Weber A., Siegel E., Kirkpatrick C.J. (2007): Actinomycosis of the jaws – histopathological study of 45 patients shows significant involvement in bisphosphonate-associated osteonecrosis and infected osteoradionecrosis. Virchows Arch, 451: 1009–1017.

Herbig A., Maixner F., Bos K.I., Zink A., Krause J., Huson D.H. (2016): MALT: Fast alignment and analysis of metagenomic DNA sequence data applied to the Tyrolean Iceman. bioRxiv doi: http://dx.doi.org/10.1101/050559.

Meyer M., Kircher M. (2010): Illumina sequencing library preparation for highly multiplexed target capture and sequencing. Cold Spring Harb Protoc: t5448, http://dx.doi.org/10.1101/pdb.prot5448.

Ortner D.J., Putschar W.G.J. (1981): Identification of pathological conditions in human skeletal remains. Smithsonian institution press, City of Washington: 218–222.

Park J.K., Lee H.K., Ha H.K., Choi H.Y., Choi C.G. (2003): Cervicofacial actinomycosis: CT and MR imaging findings in seven patients. Am J Neuroradiol, 24: 331-335.

Palfi G., Maixner F., Maczel M., Molnar E., Posa A., Kristof L.A., Marcsik A., Balazs J., Masson M., Paja L., Palko A., Szentgyörgyi R., Nerlich A., Zink A., Dutour O. (2015): Unusual spinal tuberculosis in an Avar Age skeleton (Csongrad-Felgyö, Ürmös-tanya, Hungary): A morphological and biomolecular study. Tuberculosis, 95: S29–S34.

Patil V.R., Joshi A.R., Joshi S.S., Patel D. (2014): Lumbosacral actinomycosis in an immunocompetent individual: An extremely rare case. J Craniovertebr Junction Spine, 5: 173–175.

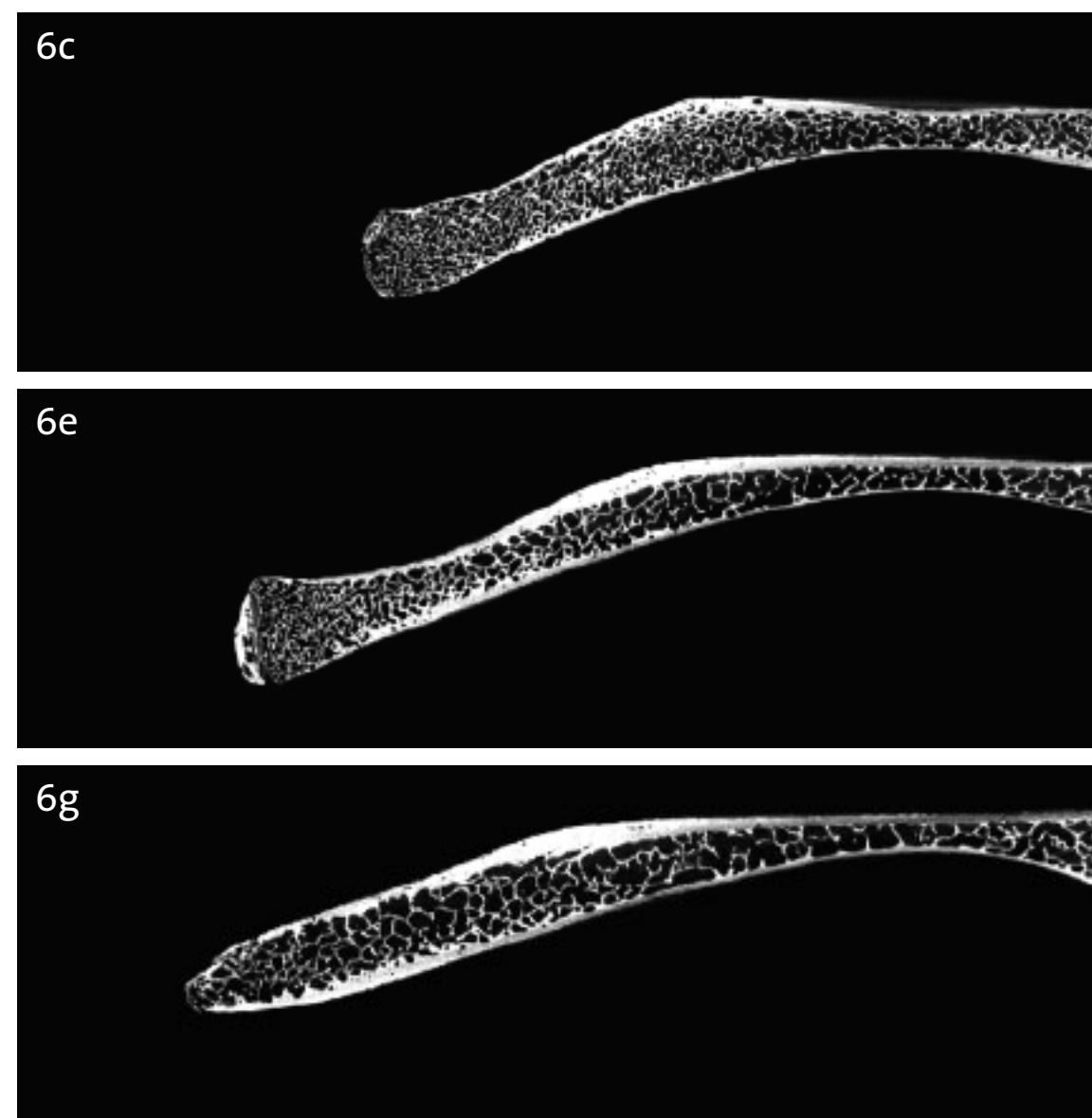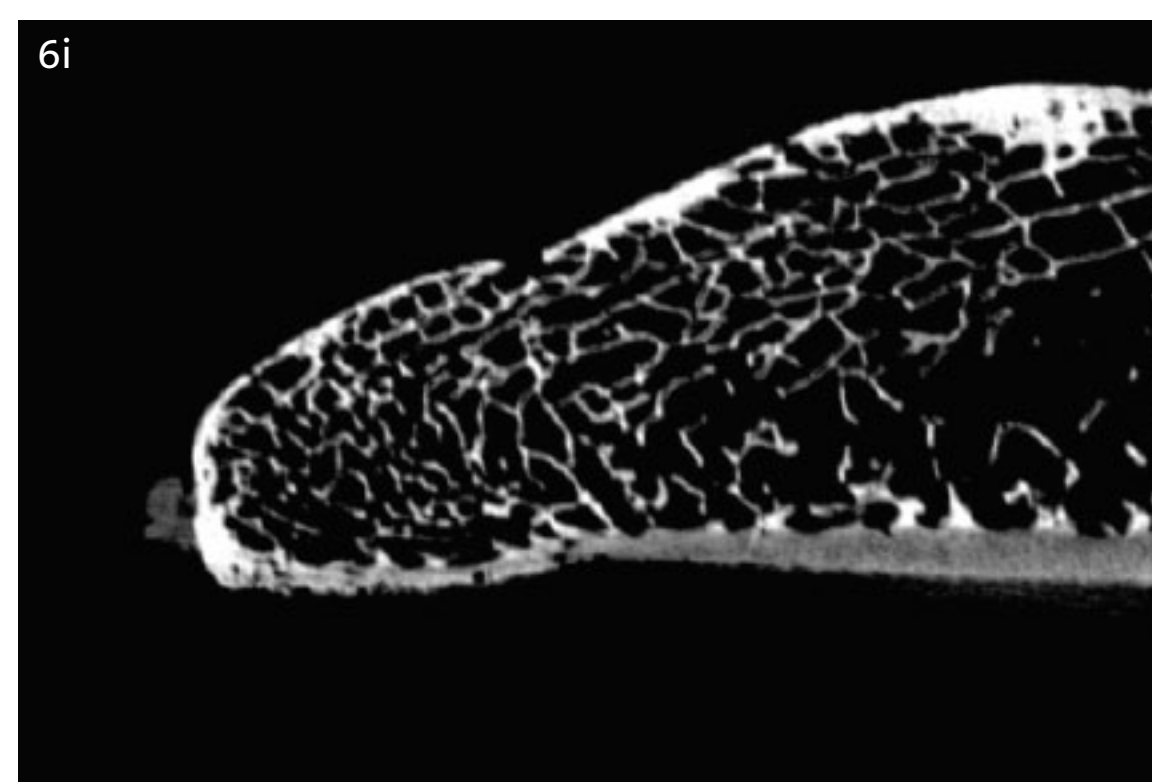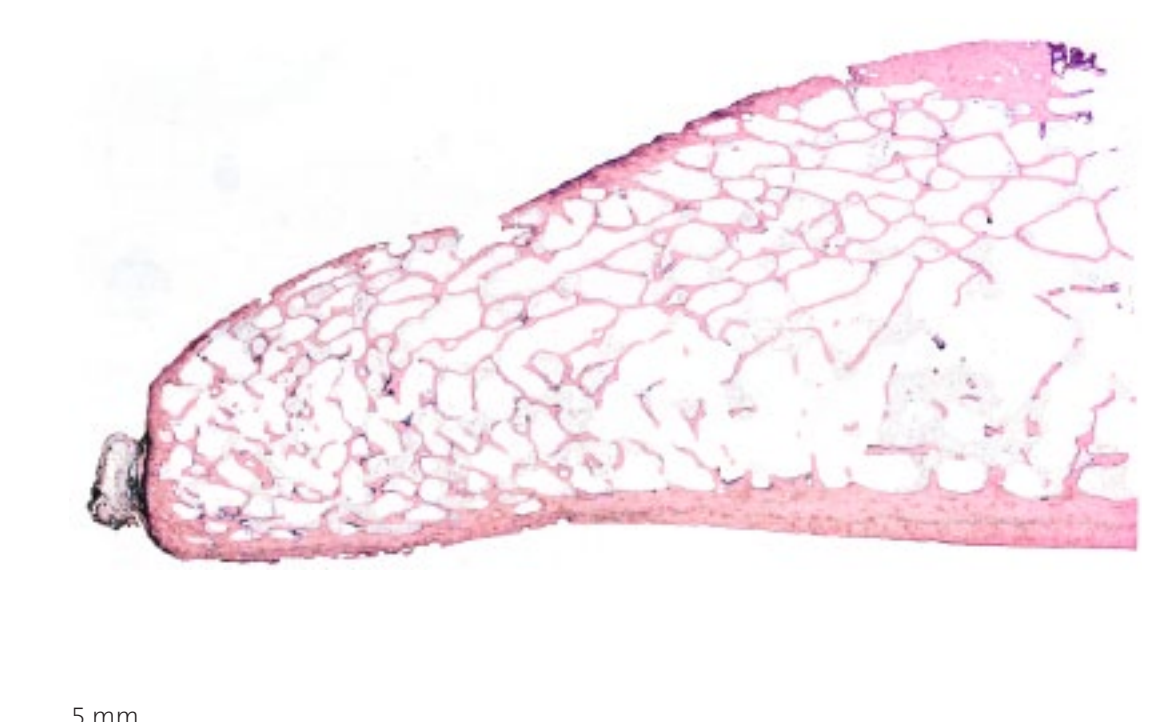Fig. 12: Macroscopical overview of the 4th and 5th lumbar vertebrae (mature male from the early Middle Ages): note the excavations as well as newly built bone with numerous perforating *Foramina* at the ventral side of the markedly deformed vertebrae.
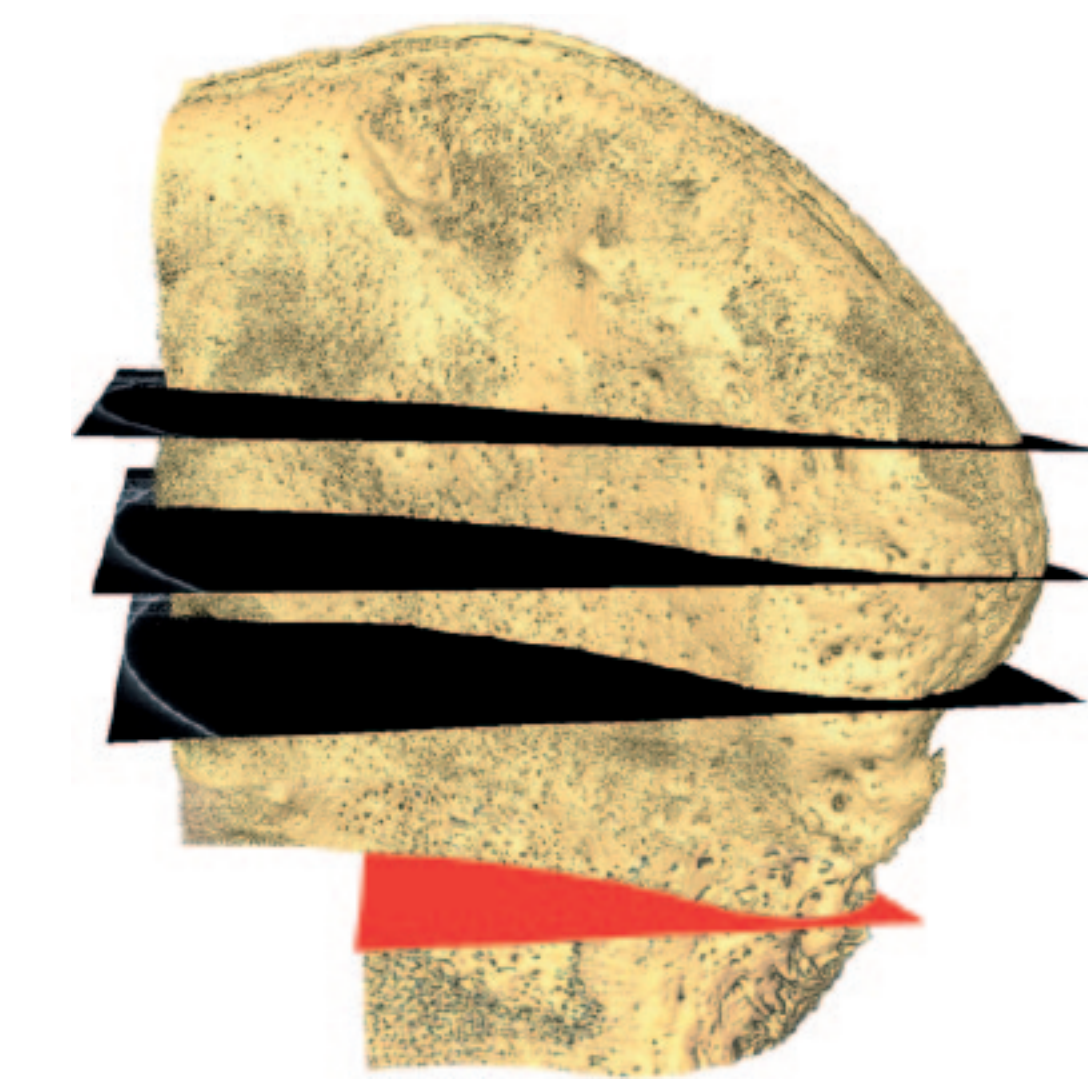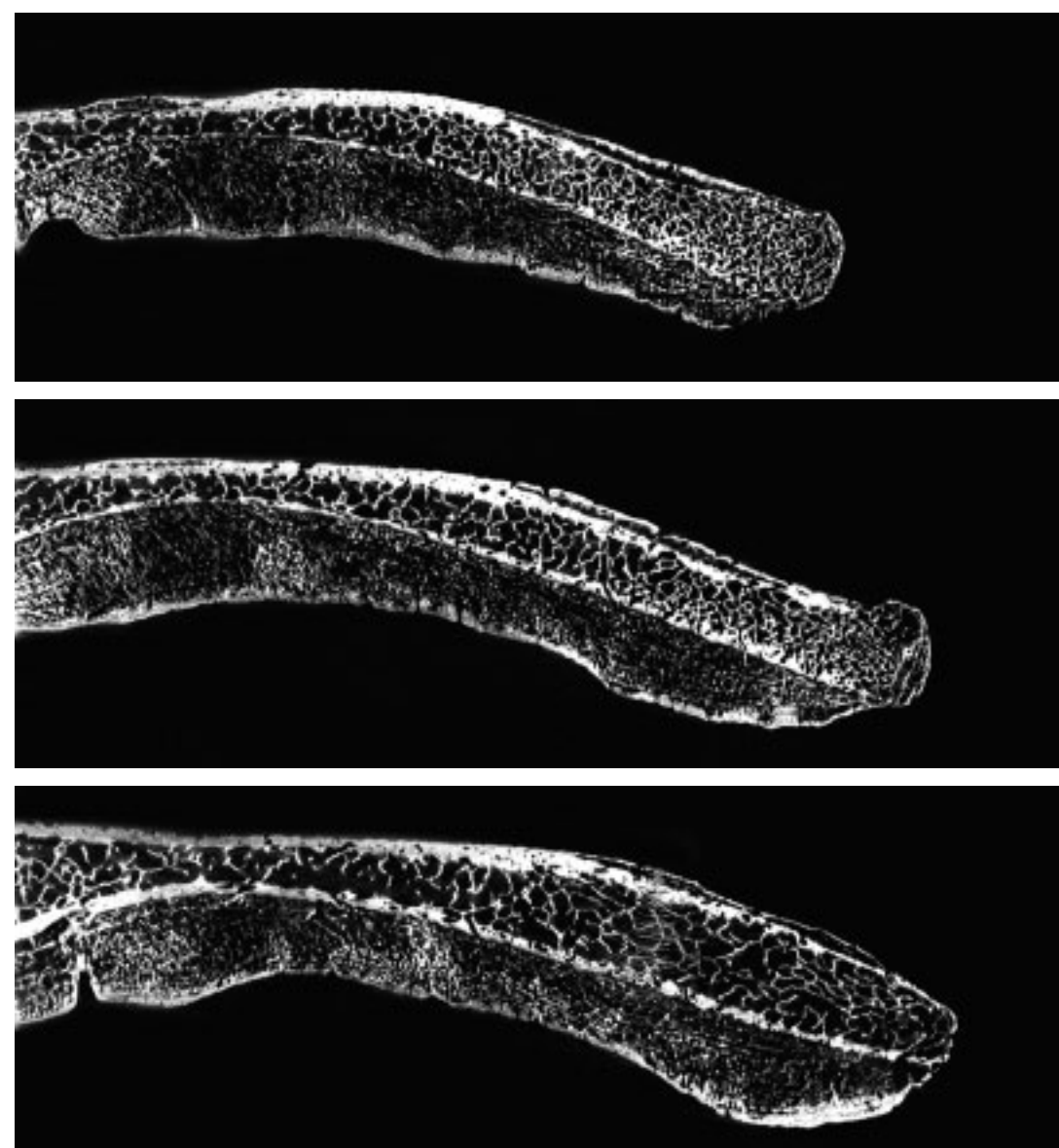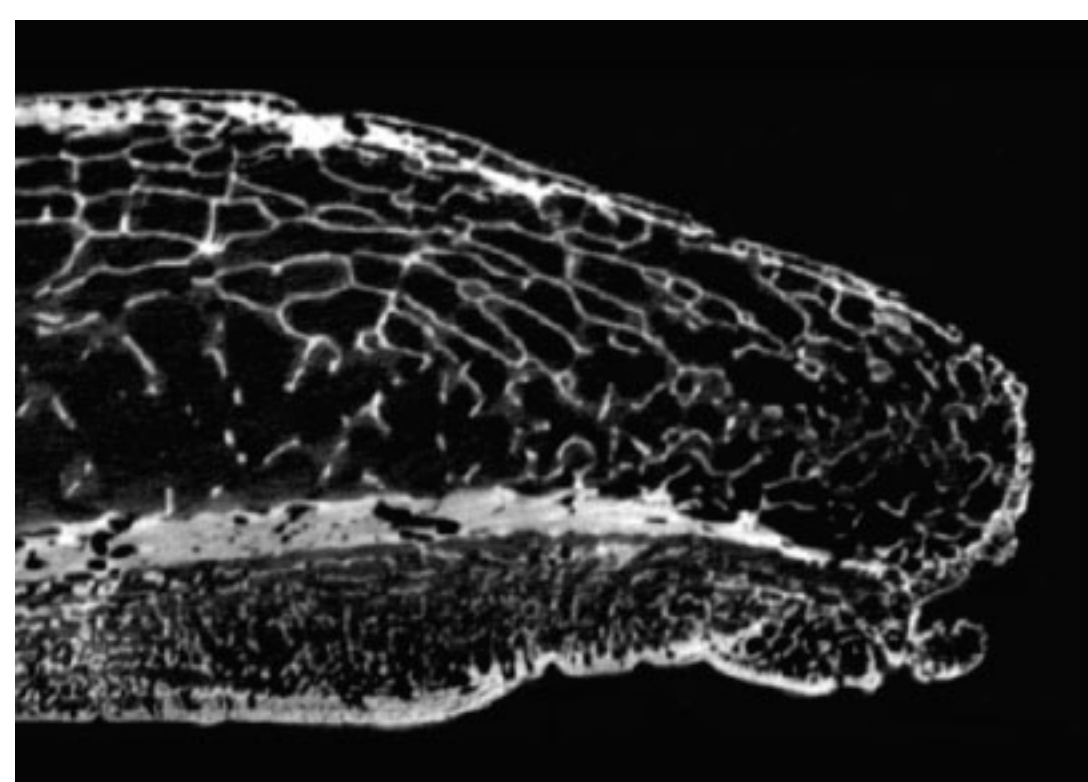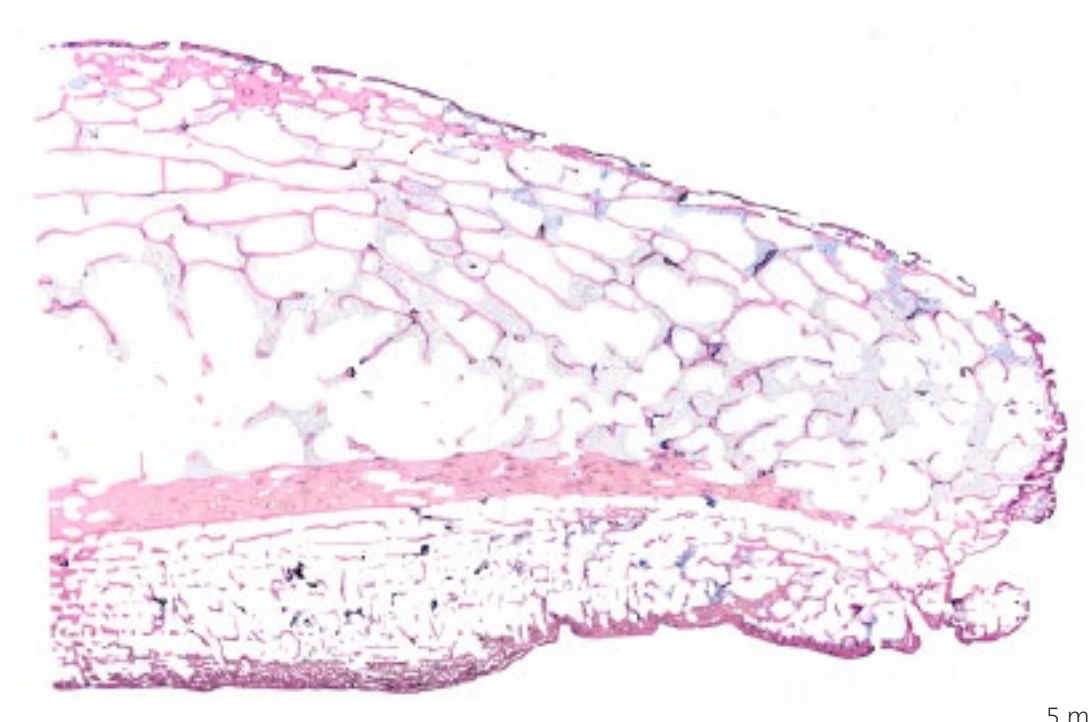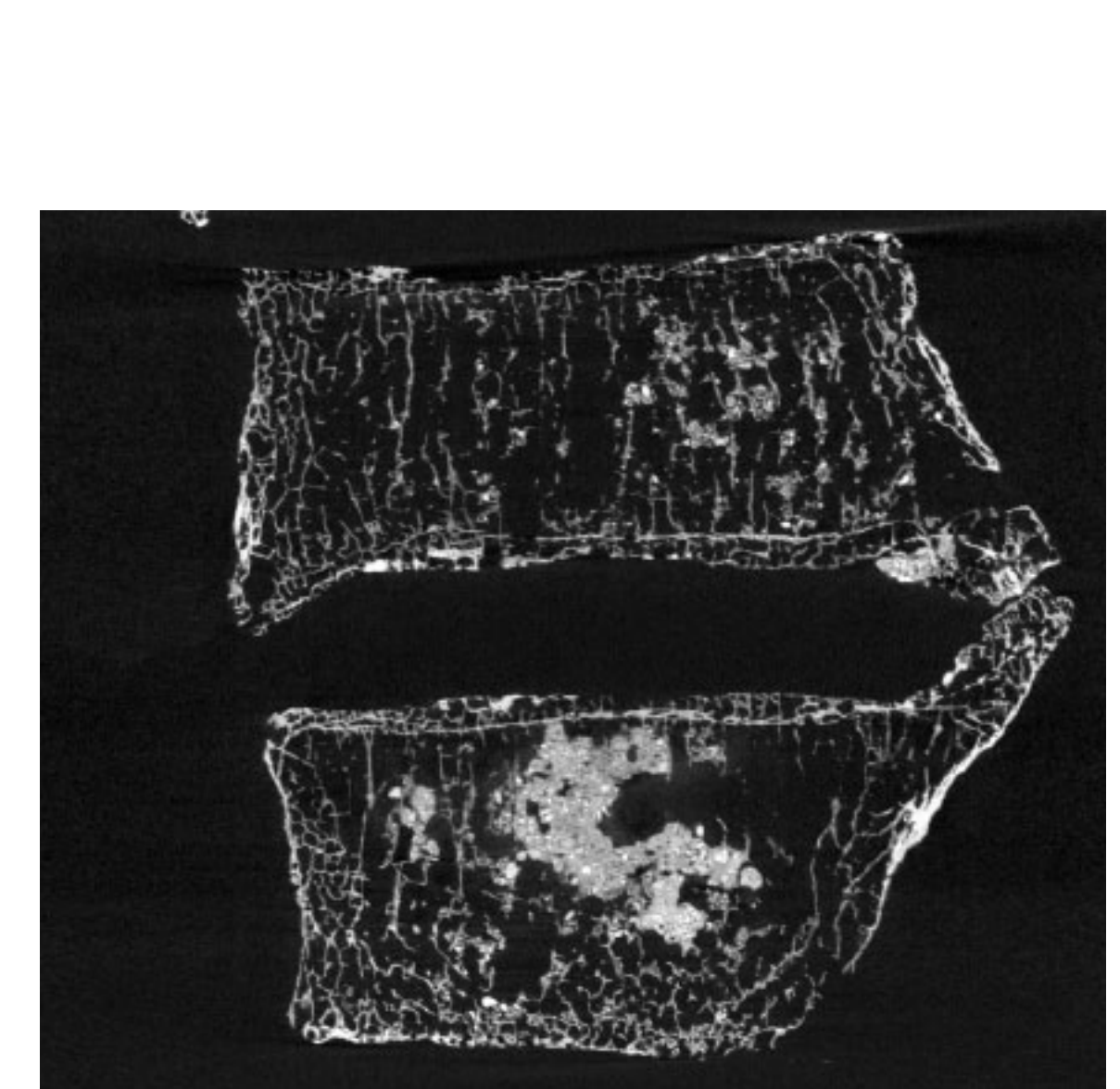

Fig 13: Radiograph of the 4th and 5th lumbar vertebrae in lateral projection (mature male from the early Middle Ages): note the cavitations also within the vertebral bodies and a coarsened trabecular network as well as hyperdense zones. The cortical contour is wedge-shaped; the periosteal bone formation is dense to a large extent and only shows few vascular channels.

Fig. 14: Single μCT plane in frontal orientation of the 4th and 5th lumbar vertebrae: note the trabecular rarefication without change of the general organisation and noteworthy signs of sclerotic response. The radiologically visible "sclerotic" areas turn out to be of post mortal origin. The eroded and split cortex seems to be strong vascularised at the endplates, but not as in plexiform bone. The new bone formation is very densely packed by irregularly arranged trabeculae.